

Supporting Information

# **Role of Protein Charge Density on Hepatitis B Virus Capsid Formation**

*Xinyu Sun,<sup>†</sup> Dong Li,<sup>†,¶</sup> Zhaoshuai Wang,<sup>§,⊥</sup> Panchao Yin,<sup>†,#</sup> Rundong Hu,<sup>‡</sup> Hui Li,<sup>†</sup> Qiao Liu,<sup>†</sup>  
Yunyi Gao,<sup>†,▽</sup> Baiping Ren,<sup>‡</sup> Jie Zheng,<sup>‡</sup> Yinan Wei,<sup>\*,§</sup> and Tianbo Liu<sup>\*,†</sup>*

*<sup>†</sup>Department of Polymer Science and <sup>‡</sup>Department of Chemical and Biomolecular Engineering,  
The University of Akron, Akron, Ohio 44325, United States*

*<sup>§</sup>Department of Chemistry, University of Kentucky, Lexington, Kentucky 40506, United States*

**This file includes:**

**Figure S1.** HBV Cp149 mutation selection and protein characterization.

**Figure S2.** CD and fluorescence spectroscopy characterization of protein with salt KCl.

**Figure S3.** Relation of HBV Cp149<sub>2</sub> capsid assembly rate with charge numbers, by using the increased scattered intensity after 1 h as a standard.

**Figure S4.** The number of capsid fractions of 1 mg mL<sup>-1</sup> of WT-0.5 M K<sup>+</sup> and 1 mg mL<sup>-1</sup> D/N-0.5M K<sup>+</sup> assemblies under matched number of charges.

**Figure S5.** Capsid aggregations observed at pH 7.0.

**Figure S6.** CD spectra of capsid proteins at various pH values.

**Table S1.** Raw data of WT Cp149<sub>2</sub> mobility measurement and effective charge calculation

Experimental details and calculations (HBV Cp149 mutation selection and protein characterization; salt effect on protein structural conformation; protein surface charge calculation and measurement; and free energy calculation for capsid formation)

## **1. HBV Cp149 mutation selection and protein characterization.**

To determine mutation sites with no potential effect on dimer association or protein folding, the protein sequence of HBV Cp 149 was carefully inspected. The 2nd and 4th Asp were selected as they are charged residues that are not involved in inter-subunit or intra-subunit salt bridge. Sodium dodecyl sulfate polyacrylamide gel electrophoresis (SDS-PAGE) and agarose gel electrophoresis verified the molecular weight and the mobility of capsid protein wild-type (WT) and mutant D2N/D4N. The Circular dichroism (CD) plot in the wavelength range of 190–250 nm reflected protein secondary structure, while the 250–400 nm range depended on protein tertiary structure. The intrinsic fluorescence of protein tracked protein folding into a tertiary structure. The CD and fluorescence traces of WT and D2N/D4N superimposed with each other, indicating that the mutations did not affect the protein structure.

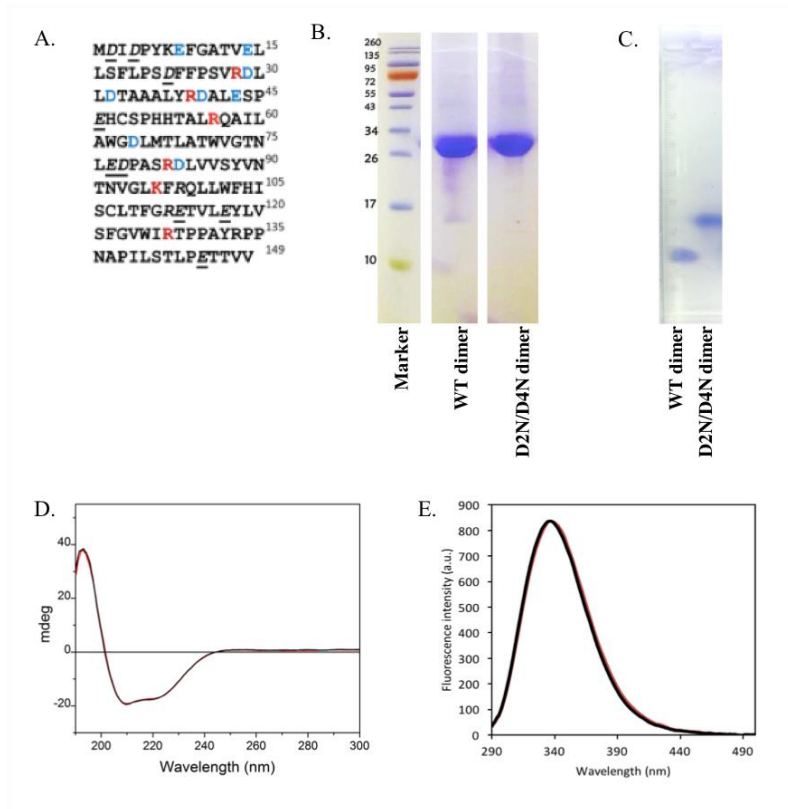


**Figure S1.** HBV Cp149 mutation selection and protein characterization. A: The protein sequence of Cp149, with residues involved in inter-subunit and intra-subunit salt bridge marked blue (negative) and red (positive). Charged residues not involved in forming salt bridge are highlighted by italic font and are underlined. B: SDS-PAGE image of WT and mutant Cp149 after purification. The molecular weight of Cp149<sub>2</sub> is ~33.5 KD. The molecular weight of band in the marker (KD) was labeled on the left of the gel. C: Agarose (1.25%) gel image tells the mobility difference between WT and D2N/D4N dimer. D2N/D4N with fewer charges travels less distance after 90 mins electrophoresis under 100V. D & E: Circular dichroism (CD) and fluorescence spectra of WT (black) and D2N/D4N (red) of Cp149<sub>2</sub>.

## 2. Salt effect on protein structural conformation.

The effect of the ion on dimer assembly was assumed to change the protein structural conformation into an “assembly-active state”.<sup>1</sup> To test this ion effect, circular dichroism was used to examine the secondary structure change of protein incubated with KCl. Both dimers were featured by 56%  $\alpha$ -helix structure, and the helix percentage almost kept constant after the titration of KCl (**Figure S2 A**). This confirmed that capsids were formed not because of the loosening of  $\alpha$ -helix bundles. From fluorescence spectra, adding monovalent salt into a high concentration of protein sample increased the fluorescence intensity without bringing a shift in the wavelength (**Figure S2 B and C**), which means the monovalent ion-induced capsid formation is not due to protein unfolding.

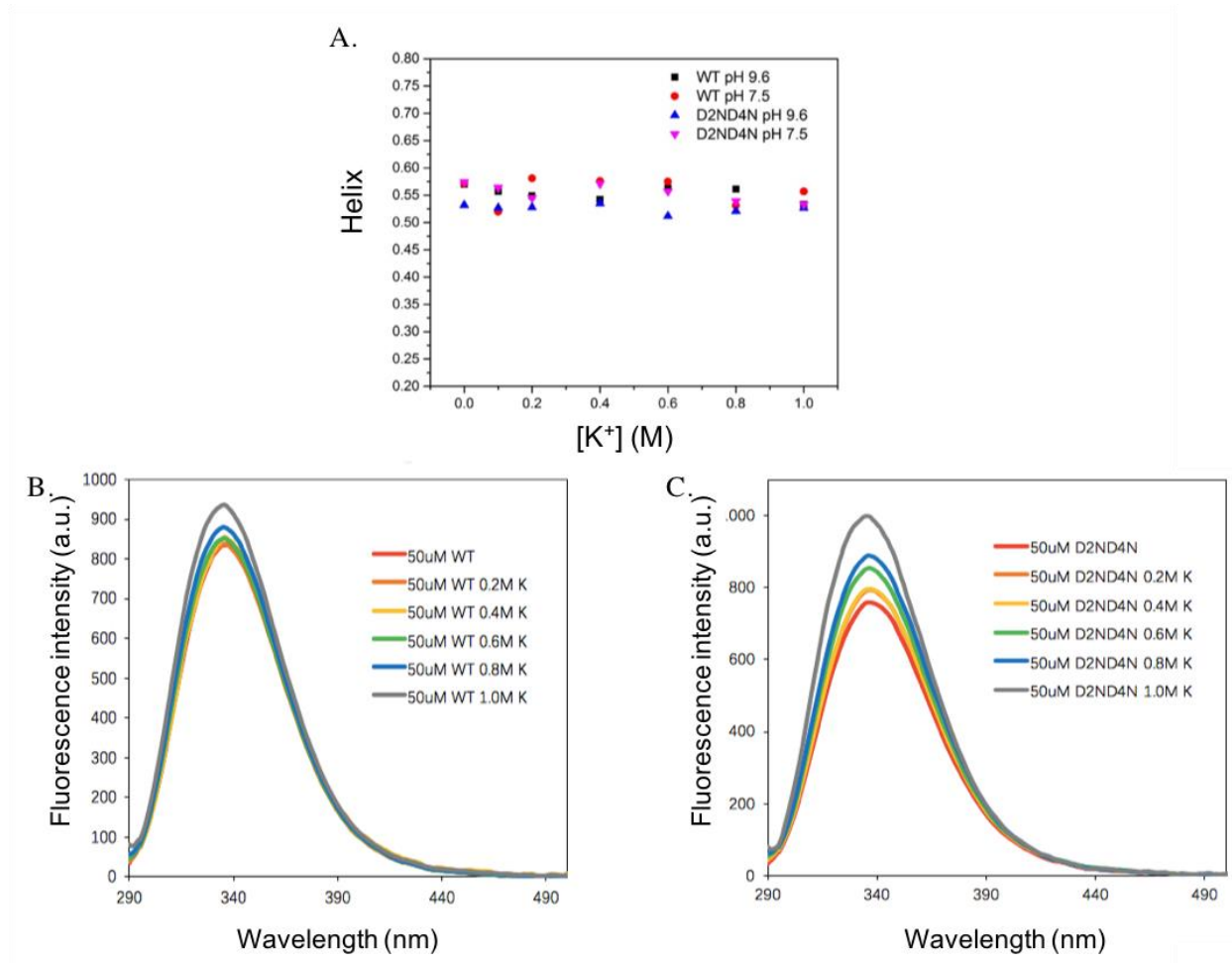


**Figure S2.** CD and fluorescence spectroscopy characterization of protein with salt KCl. A: The helix percentage of WT and D2ND4N protein kept constant with the addition of salt at pH 7.5 and pH 9.6, calculated by CD Pro using Contin method.<sup>2</sup> Wavelength from 202.4 to 260 was used for calculation to eliminate the influence of chloride salt on far UV wavelength. Protein concentration was kept well below the assembly concentration and salt was added before tests. B and C: Fluorescence spectra were taken after protein assemble into capsids with K<sup>+</sup>. The intensity increased but peak didn't shift, indicating that K<sup>+</sup> induced capsid assembly without bringing a detectable change to the protein conformation.

### 3. Protein surface charge calculation and measurement.

The protein net charges in response to pH can be obtained from an online calculator. The calculation is based on a derivation of Henderson-Hasselbalch equation:

$$Z * e = \sum_i \frac{-1}{1 + 10^{pK_{ai} - pH}} * n_i + \sum_j \frac{1}{1 + 10^{pH - pK_{bj}}} * n_j \quad (1)$$

with  $Z$  being the effective charge number;  $e$  the unit charge;  $n_i$  and  $n_j$ :  $n$  number of acidic amino acid  $i$  with an acid dissociation constant of  $pK_a$  and  $n$  number of basic amino acid  $j$  with a base constant of  $pK_b$ .

Protein effective charge can also be calculated from dimer mobility through:

$$Z * e = 6\pi\eta R_h \mu_E \frac{1 + \kappa R_h}{f(\kappa R_h)} \quad (2)$$

in which  $\eta$  is the solution viscosity;  $R_h$  is the measured hydrodynamic radius;  $\mu_E$  is the dimer mobility under an applied voltage;  $\kappa$  is the inverse Debye length and  $f(\kappa R_h)$  is Henry's function.

The Debye length was obtained through:

$$\kappa^{-1} = \sqrt{\frac{\epsilon_r \epsilon_0 k_B T}{2 N_A e^2 I}} \quad (3)$$

where  $\epsilon_0$  is the permittivity of free space;  $\epsilon_r$  is the dielectric constant;  $k_B$  is the Boltzmann constant;  $T$  is the absolute temperature in kelvins;  $N_A$  is the Avogadro number;  $e$  is the elementary charge, and  $I$  is the ionic strength.

A simple approximation formula for Henry's function  $f_o(KR_h)$  was applied to Equation S2:<sup>3</sup>

$$f_o(\kappa R_h) = 1 + \frac{1}{2 \left( 1 + \frac{2.5}{\kappa R_h (1 + 2 \exp(-\kappa R_h))} \right)^3} \quad (4)$$

The mobility of pure dimer was measured by Wyatt Mobius Zeta Potential under a voltage of 1.5 V and then substituted into Equation S2 for dimer effective charge calculation. Dimer solutions of various pHs were prepared in the same buffer as assembly study. All the measurements were performed at 22 °C.

**Table S1.** Raw data of WT Cp149<sub>2</sub> mobility measurement and effective charge calculation

	Ionic strength (mM)	$\kappa^{-1}$ (m)	Average radius (nm)	$f_o(\kappa R_h)$	Average mobility ( $\mu\text{m cm s}^{-1}\text{V}^{-1}$ )	Calculated effective charge
<b>WT pH 9.6</b>	80	1.08E-09	3.9	1.11026426	-1.575	-28.80717696
<b>WT pH 8.5</b>	16	2.41E-09	4.08	1.055648812	-1.498	-17.57482338
<b>WT pH 7.5</b>	42	1.486E-09	3.09	1.066221869	-1.14	-14.46529278

#### 4. Free energy calculation for capsid formation.

The theoretical free energy change expression was demonstrated by Adam Zlotnick and his co-workers.<sup>1,4</sup>

Briefly, considering the assembly of  $T = 4$  icosahedral capsids in which 120 dimers associate into one capsid, the equilibrium constant  $K$  can be expressed by:

$$K = \frac{[\text{capsid}]}{[\text{dimer}]^{120}} \quad (5)$$

Assuming all the contacts in the capsid are identical, this equilibrium constant can be partitioned into a single contact equilibrium constant  $K_{\text{contact}}$  by applying a statistical factor:

$$K_{\text{capsid}} = \left(\frac{j^{N-1}}{N}\right)(K_{\text{contact}})^{cN/2} \quad (6)$$

Here,  $j$ -fold degeneracy with  $N$  subunits describes the degeneracy of association based on capsid geometry, and the total number of contacts forming a capsid is  $cN/2$ , with  $N$  subunits and  $c$  number of contact surfaces per subunit. Thus, the association energy per contact can be calculated as following:

$$\Delta G_{\text{contact}} = -RT \ln(K_{\text{contact}}) \quad (7)$$

as long as the concentrations of assembled capsids and left dimers are achieved from capsid and dimer elution peak through size exclusion chromatography (SEC) separation.

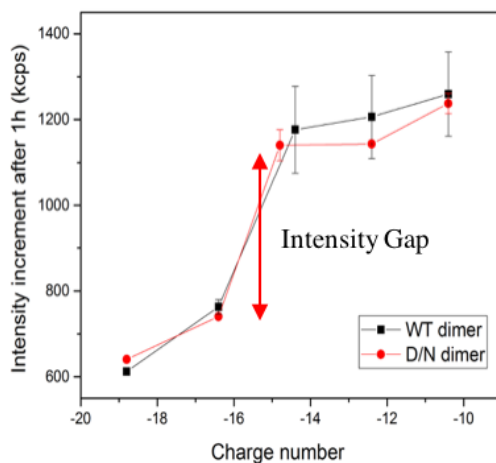


**Figure S3.** Relation of HBV Cp149<sub>2</sub> capsid assembly rate with charge numbers, by using the increased scattered intensity after 1 h as a standard.

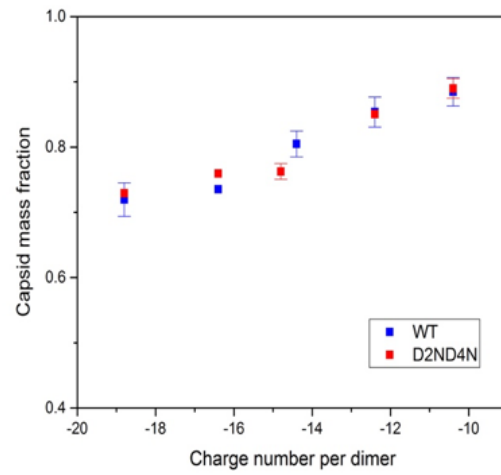


**Figure S4.** The number of capsid fractions of  $1 \text{ mg mL}^{-1}$  of WT- $0.5 \text{ M K}^+$  and  $1 \text{ mg mL}^{-1}$  D/N- $0.5 \text{ M K}^+$  assemblies under matched number of charges.

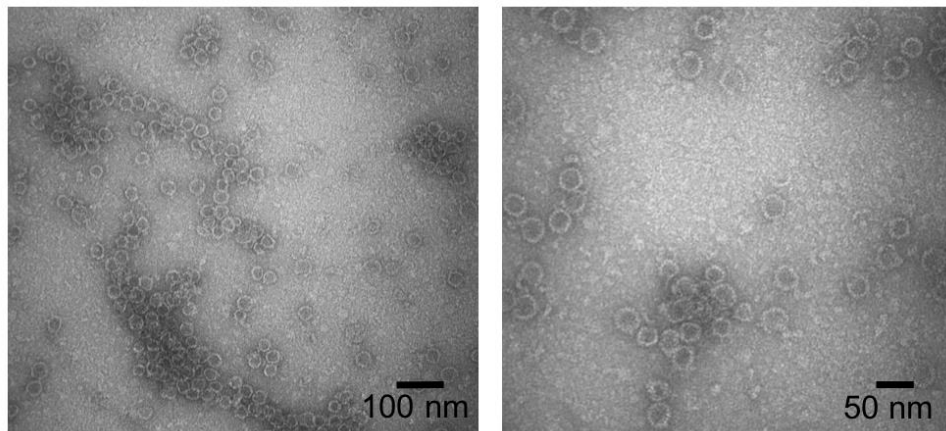


**Figure S5.** Capsid aggregations observed at pH 7.0. Assembly was conducted in  $1 \text{ mg mL}^{-1}$  D2N/D4N- $0.5 \text{ M K}^+$ .

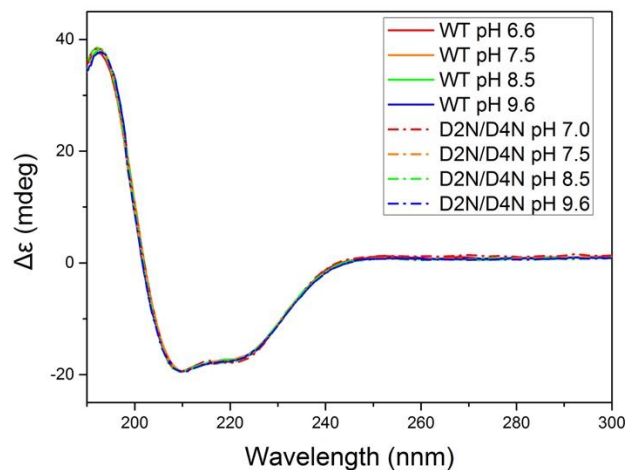


**Figure S6.** CD spectra of capsid proteins at various pH values. Two typical negative bands were stable at 220 nm and 209 nm, and a positive band was fixed at 193 nm, indicating that both WT and mutant D2N/D4N protein structures were not influenced by buffer pH.

## References:

1. Ceres, P.; Zlotnick, A., Weak protein-protein interactions are sufficient to drive assembly of hepatitis B virus capsids. *Biochemistry* **2002**, *41* (39), 11525-11531.
2. Sreerama, N.; Venyaminov, S. Y.; Woody, R. W., Estimation of protein secondary structure from circular dichroism spectra: inclusion of denatured proteins with native proteins in the analysis. *Anal. Biochem.* **2000**, *287* (2), 243-251.
3. Ohshima, H., A simple expression for Henry's function for the retardation effect in electrophoresis of spherical colloidal particles. *J. Colloid Interface Sci.* **1994**, *168* (1), 269-271.
4. Katen, S.; Zlotnick, A., The thermodynamics of virus capsid assembly. *Methods Enzymol.* **2009**, *455*, 395-417.